Translational evaluation of cytochrome P450-derived epoxyeicosanoids in non-alcoholic steatohepatitis (NASH)

Michael A. Wells, BA,[1] Kimberly C. Vendrov, BS,[1] Matthew L. Edin, PhD,[2] Brian C. Ferslew, PharmD, PhD,[1] Weibin Zha, PhD,[1] Bobbie K.H. Nguyen, BS,[1] Rachel J. Church, PhD,[3] Fred B. Lih, BA,[2] Laura M. DeGraff, BS,[2] Kim L.R. Brouwer, PharmD, PhD,[1] A. Sidney Barritt IV, MD, MSCR,[4] Darryl C. Zeldin, MD,[2] Craig R. Lee, PharmD, PhD[1]

[1]Division of Pharmacotherapy and Experimental Therapeutics, UNC Eshelman School of Pharmacy, University of North Carolina at Chapel Hill, Chapel Hill, NC.
[2]Division of Intramural Research, National Institute of Environmental Health Sciences, National Institutes of Health, Research Triangle Park, NC.
[3]University of North Carolina Institute for Drug Safety Sciences, UNC Eshelman School of Pharmacy, University of North Carolina at Chapel Hill, Chapel Hill, NC.
[4]Division of Gastroenterology and Hepatology, UNC School of Medicine, University of North Carolina at Chapel Hill, Chapel Hill, NC.

ABSTRACT

Non-alcoholic steatohepatitis (NASH) is an emerging public health problem without effective therapies. Cytochrome P450 (CYP) epoxygenases metabolize arachidonic acid into bioactive epoxyeicosatrienoic acids (EETs), which have potent anti-inflammatory and protective effects. However, the functional relevance of the CYP epoxyeicosanoid metabolism pathway in the pathogenesis of NASH remains poorly understood. Our studies demonstrate that both mice with methionine-choline deficient (MCD) diet-induced NASH and humans with biopsy-confirmed NASH exhibited significantly higher free EET concentrations compared to healthy controls. Targeted disruption of *Ephx2* (the gene encoding for soluble epoxide hydrolase) in mice further increased EET levels and significantly attenuated MCD diet-induced hepatic steatosis, inflammation and injury, as well as high fat diet-induced adipose tissue inflammation, systemic glucose intolerance and hepatic steatosis. Collectively, these findings suggest that dysregulation of the CYP epoxyeicosanoid pathway is a key pathological consequence of NASH *in vivo*, and promoting the anti-inflammatory and protective effects of EETs warrants further investigation as a novel therapeutic strategy for NASH.

Key words: non-alcoholic fatty liver disease, soluble epoxide hydrolase, CYP2J, CYP2C, epoxyeicosatrienoic acids, mice, humans

INTRODUCTION

Non-alcoholic fatty liver disease (NAFLD) is a rapidly growing public health concern that is prevalent in approximately 30% of the United States population and fueled by the diabetes and obesity epidemic (1, 2). Progression from hepatic steatosis to non-alcoholic steatohepatitis (NASH) occurs in approximately 10-20% of cases, and is characterized by progressive hepatic inflammation, injury, and fibrosis; however, the mechanisms that underlie the development and progression of this syndrome remain poorly understood (2). Furthermore, there are currently no treatments approved for the prevention or treatment of NASH (1, 2). In order to develop novel therapeutic strategies for NASH, an improved understanding of the key pathways that regulate its development and progression is needed.

Cytochrome P450 (CYP) enzymes are expressed abundantly in the liver where they are essential for the oxidative biotransformation of xenobiotics. In parallel to cyclooxygenases (COX) and lipoxygenases (LOX), certain CYP isoforms metabolize arachidonic acid to biologically active eicosanoids. Notably, CYP epoxygenase enzymes from the CYP2J and CYP2C subfamilies metabolize arachidonic acid to bioactive epoxyeicosatrienoic acids (EETs) (3). However, EETs are rapidly hydrolyzed by soluble epoxide hydrolase (sEH, *EPHX2*) to their corresponding dihydroxyeicosatrienoic acids (DHETs), which are generally less biologically active (4). CYP epoxygenase-derived EETs elicit cellular and organ protective effects in various preclinical models, including hypertension, ischemia-reperfusion injury and chemotherapy-induced organ injury, via attenuating inflammation, apoptosis and fibrosis (4-6). More recently, it has been reported that promoting the effects of EETs elicits protective effects in obesity-associated metabolic disease and in the atherogenic diet model of NAFLD/NASH in preclinical models (7-12). In addition, altered circulating CYP-derived DHET concentrations have been observed in humans diagnosed with NAFLD/NASH (13). However, the impact of NASH on EET concentrations in humans is unknown, and the functional relevance of the CYP epoxyeicosanoid metabolism pathway in the development and progression of NASH remains poorly understood.

Therefore, the objective of this study was to 1) evaluate whether EET levels are significantly altered following experimental induction of NASH in mice and in humans with biopsy-confirmed NASH; and, 2) determine whether promoting the effects of CYP epoxygenase-derived EETs attenuates the development and progression of NASH in mice.

MATERIALS AND METHODS

Reagents. Reagents were obtained from ThermoFisher Scientific (Waltham, MA) unless otherwise indicated.

Animals. All experiments were performed in adult mice on a C57BL/6J background (age 8-20 weeks). Wild-type (WT) C57BL/6J mice were purchased from Jackson Laboratory (Bar Harbor, ME). A colony of mice with targeted disruption of *Ephx2* (*Ephx2*$^{-/-}$) were backcrossed onto a C57BL/6J genetic background for more than 10 generations, as described (14, 15). All mice had free access to food and water and were housed with littermates (one to four mice per cage) in temperature and humidity controlled rooms using a 12 hour light/dark cycle. All studies were completed in accordance with the *Public Health Service Policy on Humane Care and Use of Laboratory Animals*, and were approved by the Institutional Animal Care and Use Committee at the University of North Carolina-Chapel Hill (UNC) and the National Institute of Environmental Health Sciences.

Experimental Induction of NAFLD/NASH in Mice. The first series of experiments evaluated the impact of experimental induction of NASH on hepatic and circulating CYP-derived eicosanoid concentrations in WT mice. Male WT mice were fed a commercially available methionine-choline deficient (MCD) diet (D518810, Dyets Inc., Bethlehem, PA; n=14) or a composition-matched methionine-choline replete control diet (D518754; n=10) for 4 weeks. Dietary depletion of methionine and choline leads to hepatic steatosis and oxidative stress, and subsequent liver injury, inflammation and fibrosis, and is a widely used preclinical model of NASH (16, 17). The second series of experiments evaluated the effect of disrupting sEH-mediated EET hydrolysis on MCD diet induced hepatic steatosis, injury and inflammation in male and female *Ephx2*$^{-/-}$ (n=27 [male: n=14, female: n=13]) and corresponding WT control (n=24 [male: n=8, female: n=16]) mice. A parallel group of WT mice were fed the control diet for reference (n=15 [male: n=6, female: n=9]).

The MCD diet is limited by a lack of significant weight gain and glucose intolerance (16, 17). Thus, a third series of experiments was completed to evaluate the effect of disrupting sEH-mediated EET hydrolysis on the development of obesity-associated hepatic steatosis. Male and female *Ephx2*$^{-/-}$ (n=41 [male: n=26, female: n=15]) and corresponding WT control (n=46 [male: n=33, female: n=13]) mice were fed a commercially available high-fat diet (HFD; D12492 [60% kcal fat], Research Diets Inc., New Brunswick, NJ) for 8 weeks. A parallel group of WT mice

were fed a composition-matched low-fat diet (LFD; D12450B [10% kcal fat]) for reference (n=28 [male: n=16, female: n=12]).

Body weight was measured in each mouse weekly. Food consumption was measured weekly in each cage by weighing the food at the beginning and end of each week. At the termination of each experiment, blood was collected via cardiac puncture, plasma was separated by centrifugation, and liver and epididymal white adipose tissue (eWAT) were harvested. One part of each tissue was snap-frozen in liquid nitrogen and stored at −80°C. The remainder was either fixed in 4% paraformaldehyde and embedded in paraffin or embedded in Tissue-Tek O.C.T. compound and snap-frozen in liquid nitrogen for subsequent histological analysis.

Human NASH Case:Control Study. Human samples were obtained from a single-center, case:control study of male and female patients with biopsy-confirmed NASH (n=7) and corresponding healthy volunteer controls (n=15) (18, 19). The inclusion and exclusion criteria have been described in detail previously (18). Briefly, patients with biopsy-confirmed non-cirrhotic NASH (defined as a NAFLD activity score (NAS) >3) and a BMI ≤45 kg/m^2 were recruited from the UNC hepatology clinic. In parallel, healthy volunteers with no history of hepatic or metabolic disease and a BMI ≤30 kg/m^2 were recruited from the local community. Written informed consent was obtained from all participants. The study protocol was approved by the UNC Biomedical Institutional Review Board.

Study participants fasted overnight prior to initiation of the study visit at the UNC Clinical and Translational Research Center. A blood sample was collected from an indwelling catheter at baseline and every 30 min for 2 h after administration of a standardized meal containing 509 kcal (27.2 g protein, 23.9 g fat, 53.3 g carbohydrates), as described (18, 19). Serum was separated by centrifugation, aliquoted and stored at -80°C until analysis.

Quantification of Eicosanoid Concentrations. Free eicosanoid metabolite concentrations were quantified from mouse and human samples using a targeted liquid chromatography-tandem mass spectrometry (LC/MS/MS) method with optimized sensitivity and specificity for EET quantification, as previously described (11, 12, 20). Briefly, plasma/serum (0.25 mL) and homogenized liver (20 mg) and eWAT (50 mg) tissue were diluted in 0.1% acetic acid/5% methanol solution containing 0.009 mM butylated hydroxytoluene (BHT), and internal standards were added. The samples were processed by liquid-liquid extraction to isolate lipids, and then dried. Following reconstitution, free eicosanoid metabolites were quantified by LC/MS/MS, as

described (11).

Data were acquired and concentrations were quantified with Analyst software (v1.5, Applied Biosystems) using metabolite and internal standard peaks for each sample. Tissue concentrations were normalized to tissue weight. In the human study, detectable metabolite concentrations that were <0.5x the lower limit of quantitation or >1.5x the upper limit of quantitation were imputed as such. Metabolites with more than 50% of the values outside of this range were not included in the analysis. Among the panel of 34 CYP-, COX- and LOX-derived metabolites evaluated, 24 metabolites met the criteria for analysis (Table S2). Twenty-one of the 24 metabolites (88%) had <10% of their values outside of the quantitation range.

Due to significant correlations among the EET and DHET regioisomers (11, 12, 20), the sum of the EET regioisomers (sum EETs) and DHET regioisomers (sum DHETs) were calculated to minimize redundancy. The sum of the EET and DHET regioisomers (sum EETs+DHETs) and the ratio of 14,15-EET to 14,15-DHET (14,15-EET:14,15-DHET ratio) were calculated as biomarkers of CYP epoxygenase and sEH metabolic function, respectively. Concentrations of 20-hydroxyeicosatetraenoic acid (HETE) were quantified as a biomarker of CYP omega-hydroxylase metabolic function.

Biochemical Analysis in Mice. Plasma alanine aminotransferase (ALT) levels were quantified using a Vitros 350 automated chemical analyzer (Ortho-Clinical Diagnostics, Rochester, NY). Triglyceride levels were quantified in homogenized liver tissue using the Biovision Triglyceride quantification Kit according to the manufacturer's instructions (Biovision Incorporated, Milpitas, CA).

Quantitative RT-PCR in Mice. Liver and eWAT RNA were isolated and reverse transcribed to cDNA, as described (12, 21). Expression of hepatic *Cyp2c44* (Mm0197184_m1), *Cyp2c50* (Mm00663066_gH), *Cyp2j5* (Mm00487292_m1), *Ephx2* (Mm01313813_m1), *Lpl* (Mm00434764_m1), *Col1a1* (Mm00801666_g1), *Col3a1* (Mm01254476_m1), *Srebp1* (Mm00550338_m1), *Fasn* (Mm00662319_m1) and *Scd1* (Mm00772290_m1), and eWAT *Ccl2* (Mm00441242_m1) were quantified using Taqman® Assays on Demand (Life Technologies, Foster City, CA), normalized to *Gapdh* (endogenous control, Mm99999915_g1) and expressed relative to the WT control group using the $2^{-\Delta\Delta Ct}$ method (12, 21).

MicroRNA (miR)-122 is the most abundant miRNA in hepatocytes, and is released in response to hepatocellular injury; as a consequence, circulating miR-122 levels have emerged as a sensitive biomarker of liver injury in multiple preclinical models, including MCD diet-evoked

NASH, and in humans (22, 23). Circulating miR-122 levels were quantified in the MCD diet experiments by real-time quantitative RT-PCR, as described, with minor modifications (24). Briefly, total RNA was extracted from heparinized plasma (25 µL) using the mirRNeasy serum/plasma kit (QIAGEN, Valencia, CA) according to the manufacturer's instructions. A synthetic miRNA, *Caenorhabditis elegans* miR-39 (QIAGEN, $1.6X10^8$ copies) was added to each sample during the extraction procedure. Total RNA was incubated for 1 hour at 25^0C with 1 unit of heparinase I from *Flavobacterium heparinum* (Sigma) to overcome heparin-induced enzymatic interference in PCR reactions, and then reverse transcribed using the Taqman® miRNA Reverse Transcription Kit (Life Technologies). Expression of miR-122 was quantified using a commercially-available miR-122 TaqMan® Advanced miRNA Assay (Life Technologies), normalized to *cel*-miR-39, and expressed relative to the WT control group using the $2^{-\Delta\Delta Ct}$ method (25).

ELISA in Mice. Liver tissue was homogenized and monocyte chemoattractant protein-1 (MCP-1 protein) levels were quantified in liver homogenates using the mouse CCL2/JE/MCP-1 Quantikine® ELISA kit (R&D Systems, Minneapolis, MN) after loading equal amounts of protein into each well, as described (12). Concentrations were normalized to mg of liver protein.

Histology in Mice. Embedded liver and eWAT tissue were sectioned using a serial interrupted technique (5 µm sections, 200 µm apart), as described (11, 12). Liver sections underwent hematoxylin and eosin (H&E) and Oil Red O staining, and eWAT sections underwent F4/80 immunohistochemical staining (#MCA497, AbD Serotec, Raleigh, NC). Digital images were acquired with the ScanScope CS slide capture device (Aperio, Vista, CA) and analyzed using ImageScope Version 11.1 (Aperio).

The extent of hepatic steatosis was evaluated by quantifying Oil Red O staining intensity on digital liver section images using NIH ImageJ software, as described (26). An average value across nine non-overlapping 10X fields (three fields/section x three sections/mouse) was calculated for each mouse. Data were expressed relative to the control diet referent group in each experiment. The extent of macrophage infiltration into eWAT was quantified by counting the number of crown-like structures per 10X field, as described (27). Crown-like structures were defined as a shrunken adipocyte surrounded by F4/80 stained macrophages. An average value across 15 non-overlapping fields (five fields/section x three sections/mouse) was calculated for each mouse. A pilot experiment revealed no detectable crown-like structures in female mice fed

a HFD for 8 weeks, which is consistent with prior reports in the literature (28); thus, crown-like structures were only quantified in male mice. All analyses were blinded to treatment group.

Glucose Tolerance Testing in Mice. Mice were fasted 6 hours, and then dosed with 20% D-glucose by intraperitoneal injection (2 mg/g body weight). Whole blood was collected via tail nick before and 20, 30, 60, 90 and 120 min following dosing, and blood glucose concentrations were measured using the Accu-Chek Aviva Plus Glucometer (Roche Diagnostics GmbH, Mannheim, Germany), as described (11). The area under the glucose concentration-time curve (glucose $AUC_{0\text{-}120min}$) was calculated using the trapezoidal method.

Statistical Analysis. Data are presented as mean ± standard error of the mean (SEM) unless otherwise indicated. Data that were not normally distributed were log-transformed prior to statistical analysis. Statistical analysis was performed using SAS-JMP 10.0 or SAS 9.3 software (SAS Institute, Cary, NC), and $P<0.05$ was considered significant.

In the human study, population characteristics were compared across cases and controls using student's *t*-test or Wilcoxon test for continuous variables and Fisher's exact test for categorical variables, as appropriate. In order to capture average circulating metabolite exposure over the two hour blood sampling period, the area under the eicosanoid concentration-time curve ($AUC_{0\text{-}120min}$) was calculated using the trapezoidal method. The sum EETs AUC was the primary endpoint. The sum DHETs, sum EETs+DHETs, and 14,15-EET:DHET ratio AUC's were secondary endpoints. Comparisons across cases and controls were completed using the student's *t*-test. In addition, an exploratory metabolomic analysis (student's *t*-test for each of the 24 individual metabolites followed by a false discovery rate [FDR] analysis) was performed with MetaboAnalyst v3.0, as described (20, 29).

In the mouse experiments, eicosanoid and phenotype comparisons across diet (MCD versus Control, HFD versus LFD) and genotype (*Ephx2*$^{-/-}$ versus WT) were completed using a generalized linear model (proc glm). In order to account for the potential effects of sex on the observed differences in each phenotype across experimental groups (30), the following variables were included in the model: sex, diet*sex interaction (impact of sex on the diet effect), and genotype*sex interaction (impact of sex on the genotype effect). Differences in the glucose tolerance test profile and body weight over time were evaluated using generalized linear model repeated-measures ANOVA, and a post-hoc Scheffe's test. Correlations were evaluated using Pearson correlations where indicated.

RESULTS

Experimental induction of NASH in mice increases hepatic and circulating CYP derived epoxyeicosanoids. We first investigated the effect of MCD diet administration, which evoked histologic changes consistent with the development of NASH (Fig. S1A), on free CYP-derived eicosanoid concentrations in liver. The sum EET (Fig. 1A), sum DHET (Fig. 1B), and sum EET+DHET (Fig. 1C) concentrations in liver were significantly increased in mice with MCD diet-evoked NASH compared to controls. Similar effects were seen with each EET and DHET regioisomer (Table S1). Although the hepatic 14,15-EET:DHET ratio (Fig. 1D) and hepatic 20-HETE concentrations (Fig. 1E) also appeared to be higher in MCD diet-fed mice, these differences were not statistically significant. Furthermore, liver and plasma EET concentrations exhibited a significant positive correlation ($r=0.732$, $P<0.001$), and plasma EETs were significantly increased in MCD diet-fed mice compared to controls (Fig. 1F). Similar differences were observed with the EET regioisomers and the DHET metabolites in plasma (Table S1).

Hepatic expression of key Cyp2c and Cyp2j epoxygenases was significantly reduced in the MCD diet-fed mice compared to controls (Fig. S1B). Hepatic *Ephx2* expression was also significantly suppressed in MCD diet-fed mice (Fig. S1C), and a significant inverse relationship between free hepatic EET concentrations and *Ephx2* expression was observed (Fig. S1D; $r=-0.557$, $P=0.005$). Moreover, expression of lipoprotein lipase (LpL), a key enzyme that regulates the release of esterified CYP-derived eicosanoids from lipoprotein phospholipids (31), was significantly higher in MCD diet-fed mice (Fig. S1E) and *Lpl* mRNA levels exhibited a significant positive correlation with free hepatic EET concentrations (Fig. S1F; $r=0.725$, $P<0.001$).

Patients with biopsy-confirmed NASH exhibit higher circulating CYP-derived epoxyeicosanoids compared to healthy volunteer controls. We subsequently evaluated circulating eicosanoid metabolite concentrations in a population of patients with biopsy-confirmed NASH and corresponding healthy volunteer controls. The demographic and clinical characteristics of the study population are described in Table 1. Consistent with the MCD diet preclinical model, total circulating sum EETs (Fig. 2A), sum DHETs (Fig. 2B), and sum EETs+DHETs (Fig. 2C) were significantly higher in the NASH patients compared to the healthy volunteer controls. NASH patients exhibited higher circulating sum EET, sum DHET and sum EET+DHET concentrations compared to controls over the two-hour sampling period (Fig. S2). No significant difference, however, in the 14,15-EET:DHET ratio was observed (Fig. 2D).

Evaluating the panel of 24 CYP, LOX and COX-derived metabolites (Table S2) revealed that 14,15-EET and 20-HETE were the most substantially altered circulating metabolites across cases and controls, and the only metabolites with a P-value <0.05 and a FDR q-value <0.10.

Disruption of sEH-mediated EET hydrolysis attenuates MCD diet-evoked NASH in male and female mice. Due to the observed increase in free EET levels in the presence of NASH, we sought to evaluate the functional contribution of CYP epoxygenase-derived EETs to the development and progression of NASH by administering the MCD diet to male and female *Ephx2*$^{-/-}$ mice. Consistent with the above experiments, free hepatic EETs and DHETs were higher in WT mice fed the MCD diet compared to controls (Fig. 3, Table S3). Sex did not modify the impact of the MCD diet on any metabolite in WT mice (Table S3). Consistent with disruption of sEH-mediated EET hydrolysis, MCD diet-fed *Ephx2*$^{-/-}$ mice exhibited significantly higher free EET levels, 14,15-EET:DHET ratios and 12,13-epoxyoctadecaenoic acid (EpOME): dihydroxyoctadecaenoic acid (DHOME) ratios, and significantly lower DHET levels in liver compared to MCD diet-fed WT controls (Fig. 3, Table S3). Hepatic 20-HETE concentrations, however, did not significantly differ across *Ephx2*$^{-/-}$ and WT mice (Table S3).

Administration of the MCD diet resulted in significant hepatic steatosis, injury and inflammation (Fig. 4), as well as weight loss (Fig. S3A). The increases in hepatic steatosis (Fig. 4A, Fig. S3B), plasma miR-122 and ALT levels (biomarkers of hepatocellular injury; Fig. 4B and 4C), hepatic expression of MCP-1 (a key inflammatory chemokine that regulates macrophage infiltration; Fig. 4D), and hepatic collagen expression (early biomarkers of collagen deposition and fibrosis; Fig. 4E and 4F) evoked by the MCD diet were significantly attenuated in *Ephx2*$^{-/-}$ mice. No differences in body weight (Fig. S3A), food consumption (20.8 vs. 22.6 grams/week/mouse, P=0.381), or the expression of key mediators of lipogenesis (Fig. S3C-E), were observed across *Ephx2*$^{-/-}$ and WT mice, respectively. Sex did not modify the observed differences in any phenotype across *Ephx2*$^{-/-}$ and WT mice (as evidenced by genotype*sex interaction P>0.05 for all endpoints), indicating that the protective effects of *Ephx2* disruption were similar in males and females.

Disruption of sEH-mediated EET hydrolysis attenuates HFD-evoked metabolic syndrome and NAFLD in male and female mice. Since the MCD diet is limited by a lack of weight gain, adipose tissue inflammation and glucose intolerance, which are key pathological drivers of the metabolic syndrome and NAFLD in humans (16, 17), we also evaluated the functional contribution of CYP epoxygenase-derived EETs to the development of NAFLD by administering

a HFD to male and female *Ephx2*$^{-/-}$ mice. Consistent with disruption of sEH-mediated EET hydrolysis, HFD-fed *Ephx2*$^{-/-}$ mice exhibited significantly higher 14,15-EET:DHET ratios in eWAT compared to HFD-fed WT mice (8.13±1.45 [n=12] vs. 3.05±0.62 [n=11], respectively, $P<0.05$).

Administration of the HFD for 8 weeks resulted in significant weight gain, adipose tissue inflammation, glucose intolerance and hepatic steatosis (Fig. 5, 6, and S4). The HFD-evoked increase in hepatic steatosis was significantly attenuated in *Ephx2*$^{-/-}$ mice (Fig. 5, Fig. S4D). Although no significant difference in weight gain was observed across *Ephx2*$^{-/-}$ and WT mice (Fig. 6A), *Ephx2*$^{-/-}$ mice exhibited a significantly attenuated induction of systemic glucose intolerance (Fig. 6B-D) and MCP-1 expression in eWAT (Fig. S4A) compared to WT mice. Sex did not modify the observed differences in hepatic steatosis, glucose intolerance and eWAT MCP-1 expression (genotype*sex interaction $P>0.05$ for all endpoints), indicating that the protective effects of *Ephx2* disruption were similar in males and females. Although eWAT crown-like structures were not detected in female mice, consistent with prior reports (28), the HFD-evoked increase in eWAT macrophage infiltration in male WT mice was significantly attenuated in male *Ephx2*$^{-/-}$ mice (Fig. S4B and S4C).

DISCUSSION

Nonalcoholic steatohepatitis is a rapidly growing public health concern characterized by progressive hepatic inflammation, injury, and fibrosis; however, the key pathways that regulate its development and progression remain poorly understood and no approved treatments are available (1, 2). Promoting the effects of CYP epoxygenase-derived EETs has emerged as an anti-inflammatory and protective therapeutic strategy for cardiometabolic disease (4-6). Despite the well-established pathologic role of hepatic inflammation in NASH and the abundance of CYP enzyme expression in the liver, the functional contribution of the CYP epoxyeicosanoid metabolism pathway to the pathogenesis of NASH has remained largely unexplored. Through integration of preclinical and human studies, this investigation is the first to demonstrate that 1) experimental induction of NASH in mice with the MCD diet increases free hepatic and circulating EET concentrations; 2) humans with biopsy-confirmed NASH similarly exhibit higher circulating free EET concentrations compared to healthy controls; and, 3) targeted disruption of *Ephx2* further increases free EET levels and significantly attenuates MCD diet-evoked hepatic steatosis, inflammation and injury in mice. Collectively, these findings suggest that dysregulation of the CYP epoxyeicosanoid pathway is a key pathological consequence of NASH, the observed increase in free EET concentrations may be a compensatory effect triggered to slow

the progression of NASH *in vivo*, and promoting the effects of EETs is a novel therapeutic strategy for NASH that warrants further investigation.

It is well-established that inflammatory stimuli suppress hepatic CYP-mediated xenobiotic metabolism through cytokine-mediated transcriptional downregulation of CYP expression (32). In addition, we have reported that hepatic CYP epoxygenase expression and EET biosynthesis is suppressed in mice in an LPS model of acute inflammation, a high-fat diet model of insulin resistance, and the atherogenic diet model of NAFLD (12, 21, 33). Consistent with these prior studies, experimental induction of NASH with the MCD diet significantly suppressed hepatic expression of key Cyp2c and Cyp2j epoxygenases. In contrast, the MCD diet significantly increased free hepatic and circulating EET and DHET concentrations in mice. Consistent with these preclinical data, human patients with biopsy-confirmed NASH also exhibited significantly higher circulating free EET and DHET levels compared to healthy controls. Further investigation revealed that hepatic *Ephx2* expression was suppressed in MCD diet-fed mice, and a significant inverse relationship between free hepatic EET concentrations and *Ephx2* expression was observed. Although the 14,15-EET:DHET ratio, a biomarker of reduced sEH metabolic function, appeared to be higher in MCD diet-fed mice and in human NASH patients, these differences were not statistically significant. Thus, a NASH-evoked suppression of sEH expression and EET hydrolysis did not fully account for the observed increase in EET levels. It is important to note that free eicosanoid concentrations were quantified in the current study. It is well-established that cellular EETs are esterified to membrane phospholipids and >90% of circulating EETs are esterified to lipoprotein phospholipids in humans and rodents (31, 34). Expression of LpL, an enzyme that plays a key role in release of esterified CYP-derived eicosanoids from lipoprotein phospholipids (31), was significantly higher in mice fed the MCD diet. This was consistent with a prior report, which also demonstrated that direct activation of LpL abrogates the progression of NASH (35). In the current investigation, *Lpl* mRNA levels exhibited a significant positive correlation with free hepatic EET concentrations. Taken together, these findings demonstrate that the CYP epoxyeicosanoid metabolism pathway is significantly dysregulated in the presence of NASH, and suggest that an increased release of esterified EETs may contribute, at least in part, to the observed increase in free hepatic and circulating EET concentrations.

Previous lipidomic analyses in humans have demonstrated that NAFLD/NASH is associated with dysregulated fatty acid metabolism (36, 37); however, the relationship between the presence of NASH and altered CYP-derived eicosanoids has remained largely unexplored. Due in part to the technical complexity of quantifying EETs, which are not measured on

traditional metabolomic or eicosanoid analytical platforms, major gaps in knowledge surrounding the biologic and therapeutic importance of EETs in human disease exist. A recent investigation demonstrated that circulating DHET concentrations were significantly higher in NASH patients compared to controls (13). Our analysis corroborated these findings in mice and humans, and demonstrated for the first time that free circulating EETs, but not EET:DHET ratios, are also significantly elevated in patients with NASH. During the two-hour postprandial period, circulating EET levels and the 14,15-EET:DHET ratio appeared to increase and DHET levels appeared to decrease (Figure S2). The observed increase in the 14,15-EET:DHET ratio over time in both NASH patients and healthy controls suggests that sEH metabolic function may be suppressed during the post-prandial period. To our knowledge, the effect of acute feeding on circulating CYP-derived EETs and DHETs has never been investigated in preclinical models or in humans. Future studies appear warranted to validate and elucidate these effects.

Our exploratory analysis of 24 oxylipin metabolites revealed that 14,15-EET and 20-HETE were the most substantially altered metabolites in patients with NASH. Interestingly, Loomba et al. also reported that a stable metabolite of 20-HETE (20-COOH AA) was significantly higher in NASH patients compared to controls (13). In our experiments, even though hepatic 20-HETE concentrations were not significantly altered in MCD-diet fed mice, circulating 20-HETE levels were significantly higher in MCD-diet fed WT mice compared to controls (Table S1; 1.5±0.2 vs. 0.65±0.06 ng/mL, respectively, P=0.001). Given the well-documented pro-inflammatory and pro-injury effects of 20-HETE in the cardiovascular and renal systems (38), future studies that evaluate the functional contribution of 20-HETE to the development and progression of NASH are warranted.

Although this study was the first to quantify EET and 20-HETE concentrations in human NASH patients, our analysis has limitations that must be acknowledged. First, this study was limited by its small sample size. Thus, completing sex-stratified analyses and adjusting for multiple covariates was not feasible. Second, although sum EET levels were designated as our primary endpoint, multiple secondary comparisons were completed and there is a possibility of false-positive associations. We calculated an FDR *q*-value for each comparison; however, these data should be interpreted with caution. Third, numerous potentially important eicosanoids were either below the limit of quantitation or not evaluated by the employed LC/MS/MS method. Thus, future studies in larger populations are needed to validate these preliminary findings, adjust for multiple covariates, and more rigorously evaluate the association between EETs and the presence of NASH relative to metabolites derived from parallel pathways.

It is well-established that CYP-derived EETs have potent anti-inflammatory effects by

attenuating NF-κB signaling, as well as pro-survival and anti-apoptotic effects by multiple mechanisms (4-6, 15, 39). As a consequence, promoting the effects of EETs yields vascular, myocardial, renal and cerebral protective effects in various preclinical models, including hypertension, ischemia-reperfusion injury and chemotherapy-induced organ injury via attenuation of inflammation, apoptosis and fibrosis (40-44). More recently, inhibition of sEH-mediated EET hydrolysis has been shown to abrogate obesity-associated hepatic inflammation and steatosis, atherogenic diet evoked hepatic inflammation and injury, and carbon tetrachloride induced hepatic inflammation and fibrosis (8, 12, 45). Although these accumulating data suggest that EETs and sEH are key regulators of multiple biological processes central to the pathogenesis of NAFLD/NASH, the functional role of the CYP epoxyeicosanoid metabolism pathway in the development and progression of NASH has not been rigorously studied. Using the well-established MCD diet model of NASH (16, 17), we demonstrated that mice with targeted disruption of *Ephx2* exhibited increased hepatic EET levels and significantly attenuated hepatic steatosis, pro-inflammatory chemokine expression, injury, and collagen activation. These data were consistent with the anti-inflammatory and protective effects of EETs in other models. In contrast, the expression of key mediators in the lipogenesis signaling pathway were similar in *Ephx2*$^{-/-}$ and WT mice. Taken together, these findings demonstrate that sEH is an important regulator of NASH-associated hepatic inflammation and injury, and suggest that the anti-inflammatory and cellular protective effects of EETs, and not marked alterations in lipogenesis, mediated the observed protective effects in *Ephx2*$^{-/-}$ mice. These data also suggest that the observed increase in free EET concentrations in the presence of NASH may be a compensatory effect triggered to slow the progression of NASH. Future studies are needed to establish the direct hepato-protective effects of EETs, delineate the underlying mechanisms, and further evaluate therapeutic utility of increasing EET levels in NASH.

Although the MCD diet is a well-established preclinical model that evokes hepatic inflammatory and histopathologic effects similar to human NASH, this model is limited by a lack of weight gain, adipose tissue inflammation and glucose intolerance, which are key pathological features of the metabolic syndrome and drivers of NAFLD/NASH in humans (1, 16, 17). Our experiments in a HFD model demonstrated that disruption of sEH-mediated EET hydrolysis also mitigates obesity-associated adipose tissue inflammation, systemic glucose intolerance and the early development of hepatic steatosis *in vivo*, without changes in weight gain. Given the integral role of MCP-1 expression and subsequent macrophage infiltration into adipose tissue to the obesity-associated development of glucose intolerance and type 2 diabetes, which are key pathologic drivers of NAFLD (28, 46-48), the anti-inflammatory effects of EETs in adipose tissue

appear to be a key component of their metabolic protective effects in the early stages of NAFLD. In addition, accumulating evidence has demonstrated that EETs evoke a myriad of protective effects in preclinical models of obesity, such that sEH inhibitors and EET analogs attenuate adipogenesis, pancreatic islet dysfunction, endoplasmic reticulum stress in liver and adipose tissue, and insulin resistance (7-12). Although previously published studies were completed almost exclusively in male mice, the protective effects of *Ephx2* disruption were similar in males and females in our experiments. Collectively, these data further demonstrate the potential therapeutic utility of promoting the effects of EETs in obesity-associated metabolic disease. It is important to note, however, that HFD administration for much longer durations (>6 months) is necessary to evoke hepatic inflammatory and histopathologic effects consistent with NASH (16, 17). Thus, future studies evaluating the effects of *Ephx2* disruption and novel therapies that promote the effects of EETs, including sEH inhibitors and stable EET analogs, are needed to more fully elucidate the functional contribution of CYP-derived EETs to the development and progression of obesity-associated NASH.

Despite increasing prevalence and substantial liver- and cardiovascular-related morbidity and mortality, no treatment has been approved by the FDA for NASH (1, 2). Thus, identifying and characterizing new therapeutic targets is critical. The ideal intervention for NASH would: a) elicit direct anti-inflammatory and protective effects in the liver to slow NASH progression and the development of end-stage liver disease, b) attenuate obesity-driven adipose inflammation and insulin resistance to slow the development and progression of hepatic steatosis (the most common underlying etiology of NASH), and, c) elicit systemic and vascular anti-inflammatory effects to prevent cardiovascular disease (the leading cause of death in NASH patients) (2). The anti-inflammatory and cardiovascular protective effects of EETs are well-established (4-6, 49). Importantly, sEH inhibitors are in preclinical and clinical development for chronic inflammatory conditions (50, 51). Given the metabolic and hepatic protective effects in preclinical models of obesity and NAFLD/NASH described herein, promoting the effects of EETs has enormous potential as a novel therapeutic strategy for NAFLD/NASH and warrants further investigation.

CONCLUSIONS

In summary, we have demonstrated that the CYP epoxyeicosanoid metabolism pathway is significantly dysregulated in the presence of NASH, such that free EET concentrations are significantly higher following experimental induction of NASH in mice and in patients with biopsy-confirmed NASH. In addition, genetic disruption of sEH further increased EET levels and attenuated MCD-diet induced hepatic steatosis, inflammation and injury in mice. Genetic

disruption of sEH also mitigated obesity-associated adipose tissue inflammation, systemic glucose tolerance, and the early development of hepatic steatosis. Collectively, these findings suggest that dysregulation of the CYP epoxyeicosanoid metabolism pathway is a key pathological consequence of NAFLD/NASH *in vivo*, and promoting the anti-inflammatory and protective effects of EETs offers considerable promise as a therapeutic strategy for NAFLD/NASH.

ACKNOWLEDGEMENTS

The authors gratefully acknowledge the UNC Center for Gastrointestinal Biology and Disease Cell Services & Histology Core (supported by grant P30 DK34987), the UNC Nutrition Obesity Research Center Digital Histology & Quantitative Analysis Lab (supported by grant P30 DK056350), and the UNC Department of Cell and Molecular Physiology Histology Core Facility (Kirk McNaughton, director) for their contributions to the histology analysis, and the National Institute of Environmental Health Sciences (NIEHS) Mass Spectrometry Core for their contributions to the eicosanoid metabolite analyses. This work was supported by the National Institute of General Medical Sciences of the National Institutes of Health (NIH) under Award Numbers R01 GM088199 to CRL and R01 GM041935 to KLRB, a Gateway to Research Scholarship from the American Foundation for Pharmaceutical Education to MAW, an Amgen Predoctoral Fellowship in Pharmacokinetics and Drug Disposition to BCF, the NIH National Center for Advancing Translational Sciences through Award Number 1UL1TR001111, and funds from the Intramural Research Program of the NIH/NIEHS to DCZ (Z01 ES025034). The contents of this manuscript are solely the responsibility of the authors and do not necessarily represent the official views of the NIH.

REFERENCES

1. Chalasani, N., Younossi, Z., Lavine, J. E., Diehl, A. M., Brunt, E. M., Cusi, K., Charlton, M., and Sanyal, A. J. (2012) The diagnosis and management of non-alcoholic fatty liver disease: practice Guideline by the American Association for the Study of Liver Diseases, American College of Gastroenterology, and the American Gastroenterological Association. *Hepatology* **55**, 2005-2023
2. Rinella, M. E. (2015) Nonalcoholic fatty liver disease: a systematic review. *JAMA* **313**, 2263-2273
3. Zeldin, D. C. (2001) Epoxygenase pathways of arachidonic acid metabolism. *J Biol Chem* **276**, 36059-36062
4. Imig, J. D. (2012) Epoxides and soluble epoxide hydrolase in cardiovascular physiology. *Physiol Rev* **92**, 101-130
5. Deng, Y., Theken, K. N., and Lee, C. R. (2010) Cytochrome P450 epoxygenases, soluble epoxide hydrolase, and the regulation of cardiovascular inflammation. *J Mol Cell Cardiol* **48**, 331-341
6. Oni-Orisan, A., Alsaleh, N., Lee, C. R., and Seubert, J. M. (2014) Epoxyeicosatrienoic acids and cardioprotection: the road to translation. *J Mol Cell Cardiol* **74**, 199-208
7. Luria, A., Bettaieb, A., Xi, Y., Shieh, G. J., Liu, H. C., Inoue, H., Tsai, H. J., Imig, J. D., Haj, F. G., and Hammock, B. D. (2011) Soluble epoxide hydrolase deficiency alters pancreatic islet size and improves glucose homeostasis in a model of insulin resistance. *Proc Natl Acad Sci U S A* **108**, 9038-9043
8. Liu, Y., Dang, H., Li, D., Pang, W., Hammock, B. D., and Zhu, Y. (2012) Inhibition of soluble epoxide hydrolase attenuates high-fat-diet-induced hepatic steatosis by reduced systemic inflammatory status in mice. *PLoS One* **7**, e39165
9. Sodhi, K., Puri, N., Inoue, K., Falck, J. R., Schwartzman, M. L., and Abraham, N. G. (2012) EET agonist prevents adiposity and vascular dysfunction in rats fed a high fat diet via a decrease in Bach 1 and an increase in HO-1 levels. *Prostaglandins Other Lipid Mediat* **98**, 133-142
10. Bettaieb, A., Nagata, N., AbouBechara, D., Chahed, S., Morisseau, C., Hammock, B. D., and Haj, F. G. (2013) Soluble epoxide hydrolase deficiency or inhibition attenuates diet-induced endoplasmic reticulum stress in liver and adipose tissue. *J Biol Chem* **288**, 14189-14199
11. Zha, W., Edin, M. L., Vendrov, K. C., Schuck, R. N., Lih, F. B., Jat, J. L., Bradbury, J. A., DeGraff, L. M., Hua, K., Tomer, K. B., Falck, J. R., Zeldin, D. C., and Lee, C. R. (2014)

Functional characterization of cytochrome P450-derived epoxyeicosatrienoic acids in adipogenesis and obesity. *J Lipid Res* **55**, 2124-2136

12. Schuck, R. N., Zha, W., Edin, M. L., Gruzdev, A., Vendrov, K. C., Miller, T. M., Xu, Z., Lih, F. B., DeGraff, L. M., Tomer, K. B., Jones, H. M., Makowski, L., Huang, L., Poloyac, S. M., Zeldin, D. C., and Lee, C. R. (2014) The cytochrome P450 epoxygenase pathway regulates the hepatic inflammatory response in fatty liver disease. *PLoS One* **9**, e110162
13. Loomba, R., Quehenberger, O., Armando, A., and Dennis, E. A. (2015) Polyunsaturated fatty acid metabolites as novel lipidomic biomarkers for noninvasive diagnosis of nonalcoholic steatohepatitis. *J Lipid Res* **56**, 185-192
14. Sinal, C. J., Miyata, M., Tohkin, M., Nagata, K., Bend, J. R., and Gonzalez, F. J. (2000) Targeted disruption of soluble epoxide hydrolase reveals a role in blood pressure regulation. *J Biol Chem* **275**, 40504-40510
15. Deng, Y., Edin, M. L., Theken, K. N., Schuck, R. N., Flake, G. P., Kannon, M. A., DeGraff, L. M., Lih, F. B., Foley, J., Bradbury, J. A., Graves, J. P., Tomer, K. B., Falck, J. R., Zeldin, D. C., and Lee, C. R. (2011) Endothelial CYP epoxygenase overexpression and soluble epoxide hydrolase disruption attenuate acute vascular inflammatory responses in mice. *FASEB J* **25**, 703-713
16. Takahashi, Y., Soejima, Y., and Fukusato, T. (2012) Animal models of nonalcoholic fatty liver disease/nonalcoholic steatohepatitis. *World J Gastroenterol* **18**, 2300-2308
17. Larter, C. Z., and Yeh, M. M. (2008) Animal models of NASH: getting both pathology and metabolic context right. *J Gastroenterol Hepatol* **23**, 1635-1648
18. Ferslew, B. C., Johnston, C. K., Tsakalozou, E., Bridges, A. S., Paine, M. F., Jia, W., Stewart, P. W., Barritt, A. S. t., and Brouwer, K. L. (2015) Altered morphine glucuronide and bile acid disposition in patients with nonalcoholic steatohepatitis. *Clin Pharmacol Ther* **97**, 419-427
19. Ferslew, B. C., Xie, G., Johnston, C. K., Su, M., Stewart, P. W., Jia, W., Brouwer, K. L., and Sidney Barritt, A. t. (2015) Altered bile acid metabolome in patients with nonalcoholic steatohepatitis. *Dig Dis Sci* **60**, 3318-3328
20. Oni-Orisan, A., Edin, M. L., Lee, J. A., Wells, M. A., Christensen, E. S., Vendrov, K. C., Lih, F. B., Tomer, K. B., Bai, X., Taylor, J. M., Stouffer, G. A., Zeldin, D. C., and Lee, C. R. (2016) Cytochrome P450-derived epoxyeicosatrienoic acids and coronary artery disease in humans: a targeted metabolomics study. *J Lipid Res* **57**, 109-119

21. Theken, K. N., Deng, Y., Kannon, M. A., Miller, T. M., Poloyac, S. M., and Lee, C. R. (2011) Activation of the acute inflammatory response alters cytochrome P450 expression and eicosanoid metabolism. *Drug Metab Dispos* **39**, 22-29
22. Szabo, G., and Bala, S. (2013) MicroRNAs in liver disease. *Nat Rev Gastroenterol Hepatol* **10**, 542-552
23. Clarke, J. D., Sharapova, T., Lake, A. D., Blomme, E., Maher, J., and Cherrington, N. J. (2014) Circulating microRNA 122 in the methionine and choline-deficient mouse model of non-alcoholic steatohepatitis. *J Appl Toxicol* **34**, 726-732
24. Church, R. J., Otieno, M., McDuffie, J. E., Singh, B., Sonee, M., Hall, L., Watkins, P. B., Ellinger-Ziegelbauer, H., and Harrill, A. H. (2016) Beyond miR-122: identification of microRNA alterations in blood during a time course of hepatobiliary injury and biliary hyperplasia in rats. *Toxicol Sci* **150**, 3-14
25. Kroh, E. M., Parkin, R. K., Mitchell, P. S., and Tewari, M. (2010) Analysis of circulating microRNA biomarkers in plasma and serum using quantitative reverse transcription-PCR (qRT-PCR). *Methods* **50**, 298-301
26. Mehlem, A., Hagberg, C. E., Muhl, L., Eriksson, U., and Falkevall, A. (2013) Imaging of neutral lipids by oil red O for analyzing the metabolic status in health and disease. *Nat Protoc* **8**, 1149-1154
27. Sampey, B. P., Vanhoose, A. M., Winfield, H. M., Freemerman, A. J., Muehlbauer, M. J., Fueger, P. T., Newgard, C. B., and Makowski, L. (2011) Cafeteria diet is a robust model of human metabolic syndrome with liver and adipose inflammation: comparison to high-fat diet. *Obesity* **19**, 1109-1117
28. Pettersson, U. S., Walden, T. B., Carlsson, P. O., Jansson, L., and Phillipson, M. (2012) Female mice are protected against high-fat diet induced metabolic syndrome and increase the regulatory T cell population in adipose tissue. *PLoS One* **7**, e46057
29. Xia, J., Mandal, R., Sinelnikov, I. V., Broadhurst, D., and Wishart, D. S. (2012) MetaboAnalyst 2.0--a comprehensive server for metabolomic data analysis. *Nucleic Acids Res* **40**, W127-133
30. Maric-Bilkan, C., Arnold, A. P., Taylor, D. A., Dwinell, M., Howlett, S. E., Wenger, N., Reckelhoff, J. F., Sandberg, K., Churchill, G., Levin, E., and Lundberg, M. S. (2016) Report of the National Heart, Lung, and Blood Institute Working Group on Sex Differences Research in Cardiovascular Disease: Scientific Questions and Challenges. *Hypertension* **67**, 802-807

31. Shearer, G. C., and Newman, J. W. (2009) Impact of circulating esterified eicosanoids and other oxylipins on endothelial function. *Curr Atheroscler Rep* **11**, 403-410
32. Morgan, E. T. (2001) Regulation of cytochrome p450 by inflammatory mediators: why and how? *Drug Metab Dispos* **29**, 207-212
33. Theken, K. N., Deng, Y., Schuck, R. N., Oni-Orisan, A., Miller, T. M., Kannon, M. A., Poloyac, S. M., and Lee, C. R. (2012) Enalapril reverses high-fat diet-induced alterations in cytochrome P450-mediated eicosanoid metabolism. *Am J Physiol Endocrinol Metab* **302**, E500-509
34. Spector, A. A., Fang, X., Snyder, G. D., and Weintraub, N. L. (2004) Epoxyeicosatrienoic acids (EETs): metabolism and biochemical function. *Prog Lipid Res* **43**, 55-90
35. Yu, J., Chu, E. S., Hui, A. Y., Cheung, K. F., Chan, H. L., Leung, W. K., Farrell, G. C., and Sung, J. J. (2007) Lipoprotein lipase activator ameliorates the severity of dietary steatohepatitis. *Biochem Biophys Res Commun* **356**, 53-59
36. Puri, P., Wiest, M. M., Cheung, O., Mirshahi, F., Sargeant, C., Min, H. K., Contos, M. J., Sterling, R. K., Fuchs, M., Zhou, H., Watkins, S. M., and Sanyal, A. J. (2009) The plasma lipidomic signature of nonalcoholic steatohepatitis. *Hepatology* **50**, 1827-1838
37. Feldstein, A. E., Lopez, R., Tamimi, T. A., Yerian, L., Chung, Y. M., Berk, M., Zhang, R., McIntyre, T. M., and Hazen, S. L. (2010) Mass spectrometric profiling of oxidized lipid products in human nonalcoholic fatty liver disease and nonalcoholic steatohepatitis. *J Lipid Res* **51**, 3046-3054
38. Hoopes, S. L., Garcia, V., Edin, M. L., Schwartzman, M. L., and Zeldin, D. C. (2015) Vascular actions of 20-HETE. *Prostaglandins Other Lipid Mediat* **120**, 9-16
39. Node, K., Huo, Y., Ruan, X., Yang, B., Spiecker, M., Ley, K., Zeldin, D. C., and Liao, J. K. (1999) Anti-inflammatory properties of cytochrome P450 epoxygenase-derived eicosanoids. *Science* **285**, 1276-1279
40. Hye Khan, M. A., Neckar, J., Manthati, V., Errabelli, R., Pavlov, T. S., Staruschenko, A., Falck, J. R., and Imig, J. D. (2013) Orally active epoxyeicosatrienoic acid analog attenuates kidney injury in hypertensive Dahl salt-sensitive rat. *Hypertension* **62**, 905-913
41. Manhiani, M., Quigley, J. E., Knight, S. F., Tasoobshirazi, S., Moore, T., Brands, M. W., Hammock, B. D., and Imig, J. D. (2009) Soluble epoxide hydrolase gene deletion attenuates renal injury and inflammation with DOCA-salt hypertension. *Am J Physiol Renal Physiol* **297**, F740-748

42. Sirish, P., Li, N., Liu, J. Y., Lee, K. S., Hwang, S. H., Qiu, H., Zhao, C., Ma, S. M., Lopez, J. E., Hammock, B. D., and Chiamvimonvat, N. (2013) Unique mechanistic insights into the beneficial effects of soluble epoxide hydrolase inhibitors in the prevention of cardiac fibrosis. *Proc Natl Acad Sci U S A* **110**, 5618-5623
43. Zhang, W., Otsuka, T., Sugo, N., Ardeshiri, A., Alhadid, Y. K., Iliff, J. J., DeBarber, A. E., Koop, D. R., and Alkayed, N. J. (2008) Soluble epoxide hydrolase gene deletion is protective against experimental cerebral ischemia. *Stroke* **39**, 2073-2078
44. Liu, Y., Webb, H. K., Fukushima, H., Micheli, J., Markova, S., Olson, J. L., and Kroetz, D. L. (2012) Attenuation of cisplatin-induced renal injury by inhibition of soluble epoxide hydrolase involves nuclear factor kappaB signaling. *J Pharmacol Exp Ther* **341**, 725-734
45. Harris, T. R., Bettaieb, A., Kodani, S., Dong, H., Myers, R., Chiamvimonvat, N., Haj, F. G., and Hammock, B. D. (2015) Inhibition of soluble epoxide hydrolase attenuates hepatic fibrosis and endoplasmic reticulum stress induced by carbon tetrachloride in mice. *Toxicol Appl Pharmacol* **286**, 102-111
46. Johnson, A. R., Milner, J. J., and Makowski, L. (2012) The inflammation highway: metabolism accelerates inflammatory traffic in obesity. *Immunol Rev* **249**, 218-238
47. Odegaard, J. I., and Chawla, A. (2013) Pleiotropic actions of insulin resistance and inflammation in metabolic homeostasis. *Science* **339**, 172-177
48. Weisberg, S. P., Hunter, D., Huber, R., Lemieux, J., Slaymaker, S., Vaddi, K., Charo, I., Leibel, R. L., and Ferrante, A. W., Jr. (2006) CCR2 modulates inflammatory and metabolic effects of high-fat feeding. *J Clin Invest* **116**, 115-124
49. Imig, J. D., and Hammock, B. D. (2009) Soluble epoxide hydrolase as a therapeutic target for cardiovascular diseases. *Nat Rev Drug Discov* **8**, 794-805
50. Shen, H. C., and Hammock, B. D. (2012) Discovery of inhibitors of soluble epoxide hydrolase: a target with multiple potential therapeutic indications. *J Med Chem* **55**, 1789-1808
51. Lazaar, A. L., Yang, L., Boardley, R. L., Goyal, N. S., Robertson, J., Baldwin, S. J., Newby, D. E., Wilkinson, I. B., Tal-Singer, R., Mayer, R. J., and Cheriyan, J. (2016) Pharmacokinetics, pharmacodynamics and adverse event profile of GSK2256294, a novel soluble epoxide hydrolase inhibitor. *Br J Clin Pharmacol* **81**, 971-979

FIGURES

Figure 1.

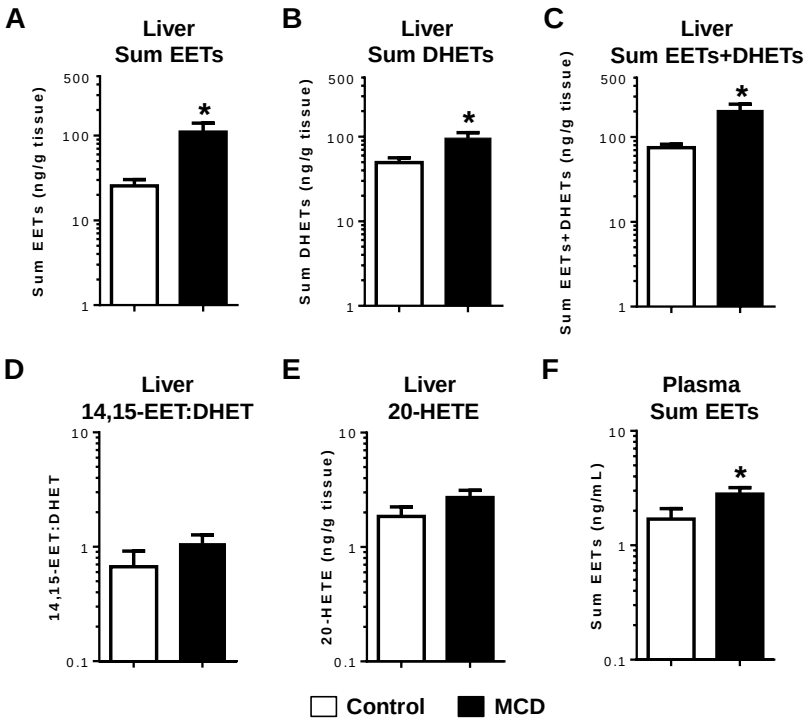

Figure 1. Hepatic and circulating CYP-derived eicosanoid concentrations in wild-type mice following experimental induction of NASH. Male mice fed the MCD diet exhibited significantly higher free hepatic (A) sum EETs, (B) sum DHETs, and (C) sum EETs+DHETs concentrations compared to mice fed a methionine-choline replete control diet (Control: n=10, MCD: n=14). In contrast, no significant differences in hepatic (D) 14,15-EET:DHET ratio or (E) 20-HETE concentrations were observed. (F) Sum EETs concentrations in plasma were also significantly higher in mice fed the MCD diet (Control: n=8, MCD: n=13). Data are presented as mean ± SEM, and are plotted on a log scale. *P<0.05 versus control.

Figure 2.

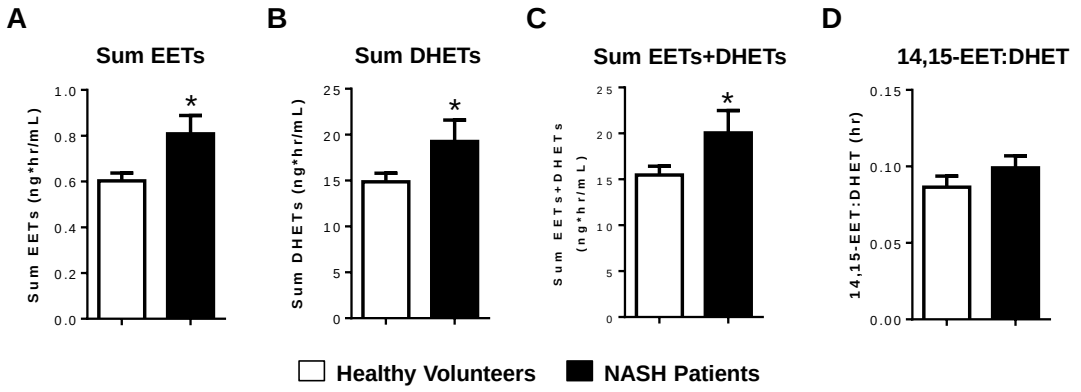

Figure 2. Circulating CYP epoxygenase-derived eicosanoids in a human population of patients with biopsy-confirmed NASH and healthy volunteer controls. Free serum eicosanoid concentrations were quantified at baseline (fasting) and at 0.5, 1.0, 1.5 and 2.0 hours following administration of a standardized meal. In order to quantify the average circulating metabolite exposure over the two hour blood sampling period, the area under the concentration-versus-time curve ($AUC_{0\text{-}120min}$) was calculated for each metabolite and compared across NASH cases (n=7) and healthy volunteer controls (n=15). The (A) sum EETs, (B) sum DHETs, and (C) sum EETs+DHETs AUC were significantly higher in NASH patients versus healthy volunteer controls. (D) No significant difference in the 14,15-EET:DHET AUC was observed. Data are presented as mean ± SEM. *P<0.05 versus healthy volunteers.

Figure 3.

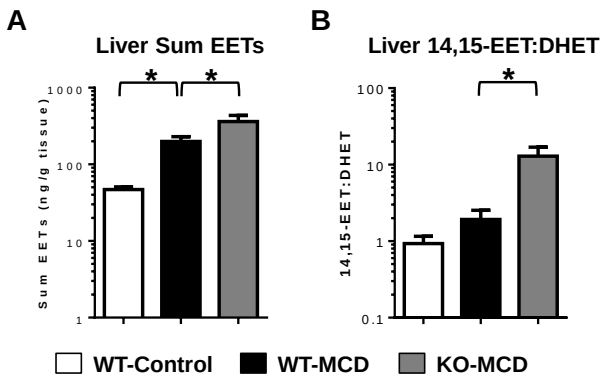

Figure 3. Hepatic CYP-derived eicosanoid concentrations in *Ephx2*$^{-/-}$ mice following experimental induction of NASH. (A) Sum EET levels and (B) the 14-15-EET:DHET ratio in liver were quantified in male and female wild-type (WT) and *Ephx2*$^{-/-}$ mice. Compared to WT mice fed a control diet for 4 weeks (WT-Control, n=11), WT mice fed the MCD diet (WT-MCD, n=15) exhibited significantly higher hepatic sum EET levels, whereas no significant difference in the 14,15-EET:DHET ratio was observed. *Ephx2*$^{-/-}$ mice fed the MCD diet (KO-MCD, n=12) exhibited significantly higher EETs and 14,15-EET:DHET ratio compared to WT-MCD. Data are presented as mean ± SEM, and are plotted on a log-linear scale. *P<0.05 versus WT-MCD.

Figure 4.

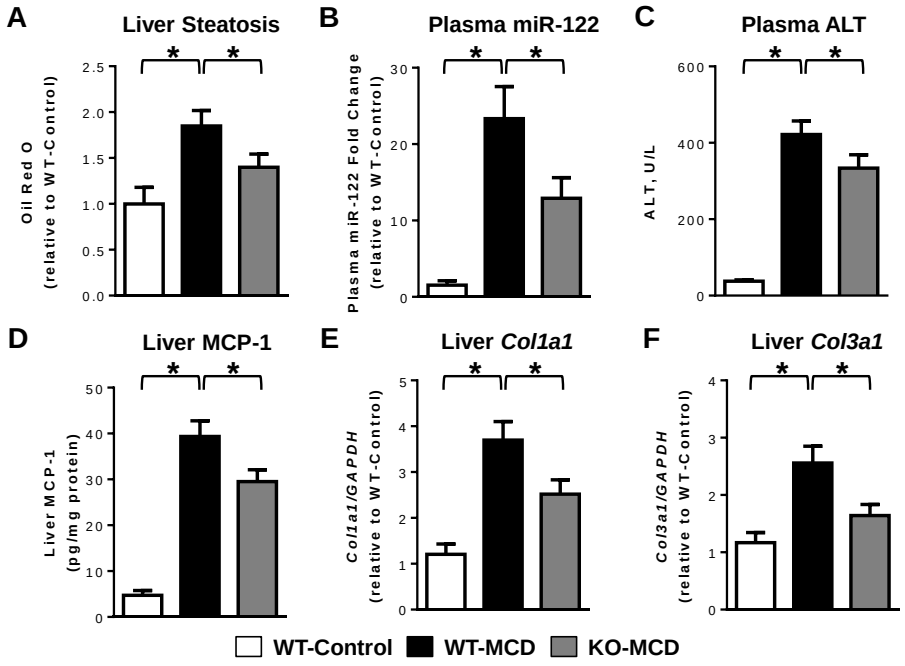

Figure 4. Phenotypic characteristics of NASH in *Ephx2*$^{-/-}$ mice following experimental induction of NASH. Male and female mice were fed a methionine-choline deficient (MCD) or methionine-choline replete control diet for 4 weeks to induce NASH. The MCD diet-evoked increases in (A) histologic evidence of hepatic steatosis (measured by Oil Red O staining in serial interrupted liver sections; representative images are provided in Figure S3B) and (B) plasma miR-122 levels in wild-type (WT) mice were significantly attenuated in *Ephx2*$^{-/-}$ (KO) mice (WT-Control: n=8; WT-MCD: n=14-17; KO-MCD: n=16-19). The MCD diet-evoked increases in (C) plasma ALT levels, (D) hepatic MCP-1 levels, and hepatic mRNA levels of (E) collagen type I (*Col1a1*) and (F) collagen type III (*Col3a1)* also were attenuated in *Ephx2*$^{-/-}$ mice (WT-Control: n=14-15; WT-MCD: n=24; KO-MCD: n=25-27). Data are presented as mean ± SEM. *P<0.05 versus WT-MCD.

Figure 5.

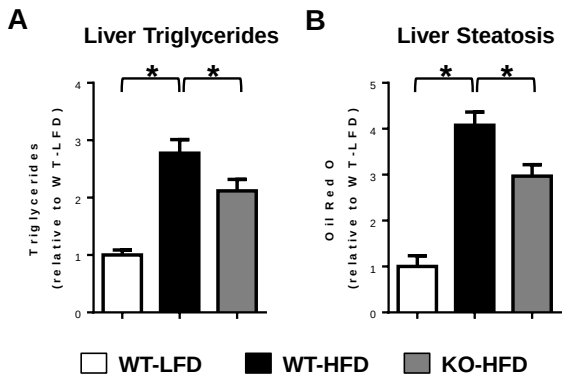

Figure 5. Hepatic steatosis in *Ephx2*$^{-/-}$ mice following experimental induction of obesity. Male and female mice were fed a high-fat diet (HFD) for 8 weeks to induce obesity and hepatic steatosis. (A) The HFD-evoked increase in liver triglyceride levels in wild-type (WT) mice was significantly attenuated in *Ephx2*$^{-/-}$ (KO) mice (WT-LFD: n=8; WT-HFD: n=22; KO-HFD: n=23). (B) Histologic evidence of hepatic steatosis, which was measured by Oil Red O staining in serial interrupted liver sections (representative images are provided in Figure S4D), was also attenuated in *Ephx2*$^{-/-}$ mice (WT-LFD: n=10; WT-HFD: n=11; KO-HFD: n=12). Data are presented as mean ± SEM. *P<0.05 versus WT-HFD.

Figure 6.

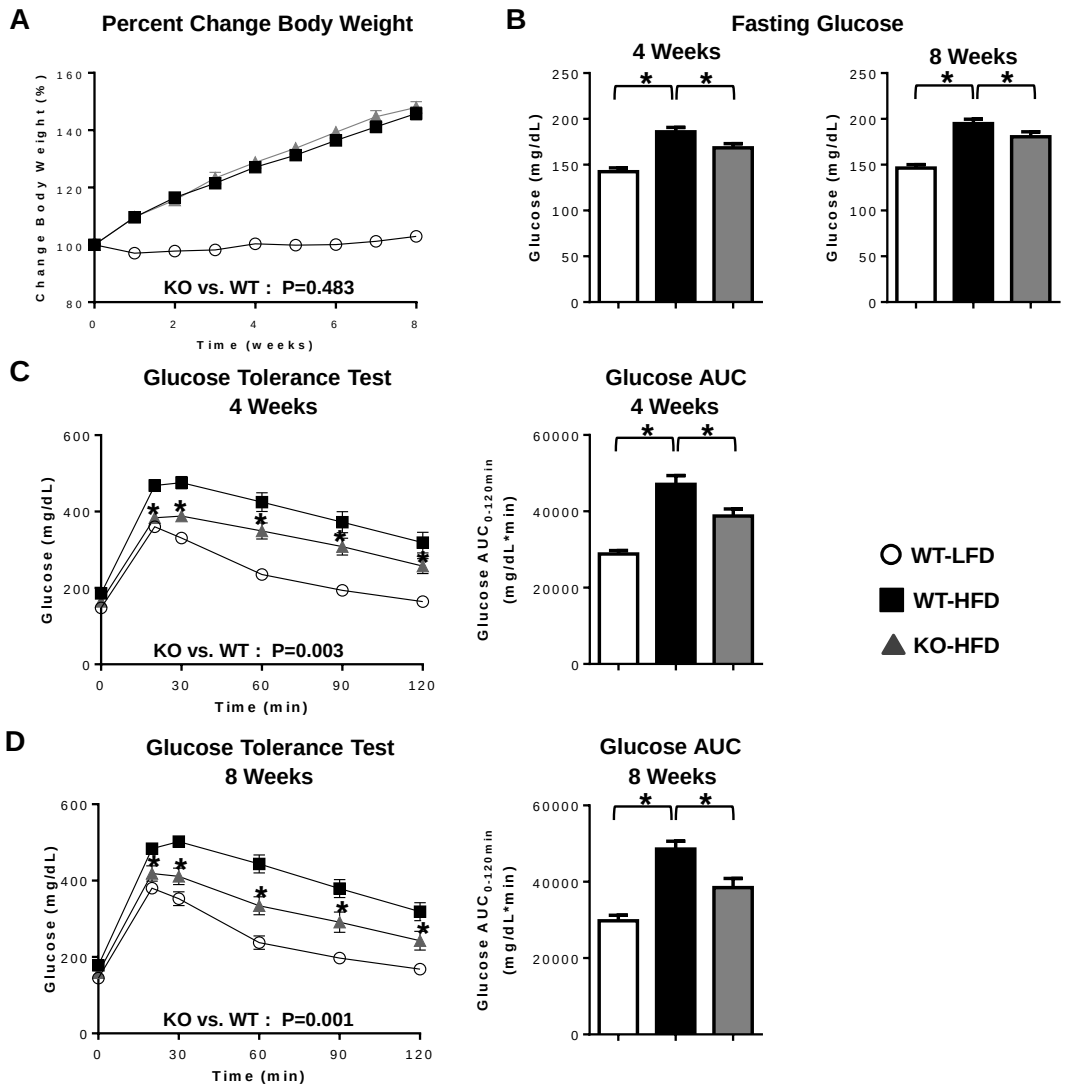

Figure 6. Glucose intolerance in *Ephx2*$^{-/-}$ mice following experimental induction of obesity. Male and female mice were fed a high-fat diet (HFD) for 8 weeks to induce obesity and glucose intolerance. (A) Body weight was measured weekly and expressed as a percent change from baseline, and (B) fasting blood glucose levels were measured at 4 and 8 weeks (WT-LFD: n=28; WT-HFD: n=44-46; KO-HFD: n=41). At (C) 4 weeks (WT-LFD: n=22; WT-HFD: n=32; KO-HFD: n=32) and (D) 8 weeks (WT-LFD: n=16; WT-HFD: n=23; KO-HFD: n=23), blood glucose concentrations were quantified over 120 minutes following an intraperitoneal glucose tolerance test (GTT). The corresponding glucose $AUC_{0\text{-}120min}$ was then calculated. The repeated measures ANOVA P-values are provided where applicable. *P<0.05 versus WT-HFD.

TABLES

Table 1. Study population characteristics[a]

Characteristic	Healthy volunteers (n=15)	NASH Patients (n=7)	P-value[b]
Demographics			
Age (years)	43.1 ± 12.5	48.1 ± 10.4	0.333
Male	7 (46.7%)	3 (42.9%)	1.000
African American	2 (13.3%)	0 (0.0%)	1.000
BMI (kg/m^2)	25.3 ± 2.7	32.2 ± 5.2	0.011
Serum Chemistry (fasting)			
ALT (u/L)	28 [23-41]	55 [46-100]	0.001
Total Cholesterol (mg/dL)	182 [162-234]	220 [157-228]	0.972
Triglycerides (mg/dL)	81 [46-154]	247 [190-286]	<0.001
Glucose (mg/dL)	84 [82-94]	125 [104-138]	<0.001
Insulin (µIU/mL)	7.5 [5.8-9.4]	29.5 [16.2-54.3]	<0.001
Liver Histology			
Total NAS[c]	-	5 [4-6]	
Steatosis	-	2 [1-3]	
Ballooning	-	2 [0-2]	
Inflammation	-	1 [0-2]	
Fibrosis	-	1 [0-3]	

Data presented as mean ± standard deviation, median [interquartile range], or count (%)

ALT, alanine aminotransferase; BMI, body mass index; HDL, high density lipoprotein; NAS, NAFLD Activity Score

[a]These data have been previously reported (19)

[b]Student's *t*-test or Wilcoxon test was performed for continuous variables and Fisher's exact test was performed for categorical variables, as appropriate.

[c]NAS is a validated histological scoring system that includes four distinct domains. The total (sum) score and the score for each domain are provided for the NASH patients (liver biopsies were not completed in healthy volunteers).